Journal of Catalysis 269 (2010) 103–109

Contents lists available at ScienceDirect

Journal of Catalysis

journal homepage: www.elsevier.com/locate/jcat

Ni-ZSM-5 catalysts: Detailed characterization of metal sites for proper catalyst design

A.J. Maia [a], B. Louis [b], Y.L. Lam [c], M.M. Pereira [a,*]

[a] Universidade Federal do Rio de Janeiro, Centro de Tecnologia, Departamento de Química Inorgânica, Avenida Athos da Silveira Ramos, 149, Ilha do Fundão, 21941-909, Rio de Janeiro, RJ, Brazil
[b] Laboratoire des Matériaux, Surfaces et Procédés pour la Catalyse (LMSPC), European Laboratory for Catalysis and Surface Science (ELCASS), UMR 7515 du CNRS Université de Strasbourg, 25 Rue Becquerel, 67087 Strasbourg Cedex 2, France
[c] PETROBRAS, Centro de Pesquisas e Desenvolvimento Leopoldo A. Miguez de Mello (CENPES), PDAB, Tecnologia em FCC, 21949-900, Ilha do Fundão, Rio de Janeiro, RJ, Brazil

ARTICLE INFO

Article history:
Received 31 August 2009
Revised 14 October 2009
Accepted 24 October 2009
Available online 26 November 2009

Keywords:
Nickel
ZSM-5
n-Hexane cracking
Ethylene selectivity

ABSTRACT

Nickel was introduced in ZSM-5 zeolite by two different methods: dry impregnation and ionic exchange. Different loadings of metal, ranging from 0.4 to 6 wt% were explored. These materials were thoroughly characterized by EXAFS, TPR, acidity measurements by H/D isotope exchange and ethane hydrogenolysis. Regardless of the metal introduction method, at 0.4 wt% Ni, the Ni-ZSM-5 catalysts present only nickel located inside the zeolite channels as compensation cations. In contrast, an increase to 1 wt% nickel (via impregnation) led to its presence both inside and outside the channels.

The catalytic activity of these Ni-ZSM-5 zeolites was tested in *n*-hexane cracking. Depending on the way the metal was introduced, it was possible to modify the *n*-hexane cracking activity and the selectivity toward light alkenes. Hence, a proper design of metal and acid sites could be achieved.

1. Introduction

Nickel-based catalysts have been extensively studied during the past decades [1,2]. While Ni contamination generally produces undesirable hydrogen and high coke yields in the fluid catalytic cracking (FCC) process, zeolites containing low loadings in metals are reported to be particularly attractive additives in the FCC process in the NOx reduction during the regeneration process [3].

Acid-catalyzed transformations of hydrocarbons such as cracking and isomerization are of prime importance [4]. The chemical inertness of the starting alkanes is generally overcome by the use of high temperatures and strongly acidic catalysts such as H-zeolites [5]. These hydrogen atoms localized in the zeolite as compensation cations can be substituted by other ions. Particularly, divalent metal ions could not only be distributed as isolated species, but also form small oligomers or even particles in analogy to more condensed nickel (II) species in an aqueous solution [6].

Transition metal ions are usually introduced in the support by ion exchange, pH-controlled precipitation or dry impregnation. The latter remains the most used method to prepare supported nickel catalysts. Indeed, most of nickel ions are dispersed on the outer surface and, in contrast, fewer ions are distributed as compensation cations according to the literature [7,8]. Particularly on zeolites, the questions associated to the formation of active metallic sites may become very complex once the various possibilities of metal ion localization [9,10], the metallic diffusion and its sintering throughout the framework [11] affect the catalyst.

The structure and properties of small metallic particles supported on oxides and zeolites continue to attract considerable attention [12,13]. There is currently a great interest toward the understanding of electronic and catalytic properties of these systems as well as in the basic processes involved in the formation of stable metallic nanoparticles [14]. Model systems in which nickel was introduced in micro-, meso- and macroporous supports have therefore been developed [15,16]. Unfortunately, these studies were often done at high nickel content, in contrast with low metal contents usually found in the FCC catalyst. Furthermore, due to the particular reaction/regeneration conditions of the FCC process, nickel is present in different oxidation states and not only as zero oxidation state (metallic site). Recently, model systems with nickel content at the parts per milium (ppm) level have been studied in order to understand the reasons for FCC catalyst poisoning [17–19]. The different possibilities of nickel location and distribution in the zeolite cages and channels can also affect the acid properties of the porous host. Nickel particle is active by itself for several catalytic reactions, as proposed by Boudart and Djega [20]. By controlling the nickel particle size, one can favor dehydrogenation products instead of hydrogenolysis products [21]. The combination of metal sites, which can be of different oxidation

* Corresponding author. Fax: +55 2125627106.
E-mail address: maciel@iq.ufrj.br (M.M. Pereira).

0021-9517/$ - see front matter © 2009 Elsevier Inc. All rights reserved.
doi:10.1016/j.jcat.2009.10.021

states with the zeolite acid sites led to a fascinating topic in catalysis: the bi-functional catalyst. Thus, in order to improve olefin production, the hydrocarbon activation could be tailor-made by controlling the nature of the nickel species, their distribution in the zeolite and the amount of zeolite acid sites. Hence, more attention has to be paid to clarify their catalytic behavior. Whereas, the metal is active to promote several reactions [22–24], its presence may also influence the sequence of acid-catalyzed transformations occurring within the zeolite.

Based on several physical techniques, a complete characterization of nickel ZSM-5 zeolite was made to investigate the state of nickel and also the zeolite acidity. Cracking of *n*-hexane was performed to probe the bifunctional behavior of these catalysts. The understanding of the influence of the preparation procedure for metal introduction (dry impregnation versus ionic exchange), its final distribution, and the zeolite acidity will be useful to achieve a proper design of Ni-HZSM-5 bifunctional catalyst.

2. Experimental

2.1. Ni-ZSM-5 catalysts preparation

The ZSM-5 zeolite was prepared as described elsewhere [25]. The Si/Al ratio was determined by chemical analysis and the SiO_2/Al_2O_3 molar ratio of HZSM-5 was 25. In addition, solid state ^{27}Al MAS NMR showed only tetrahedral aluminum species due to framework sites.

Nickel-zeolite catalysts were synthesized according to two different methods for metal introduction. Different levels of metal loadings were used: 0.4; 1; 4, and 6 wt%. Dry impregnation procedure was performed with nickel carboxylate as a precursor in toluene as described elsewhere [26]. This procedure tends to suppress nickel ion exchange into the zeolite cages. The deposition was carried out in a rotary evaporator for 30 min at an ambient temperature. The catalyst was dried for 1 h under vacuum at 120 °C and then calcined in air at 600 °C for 3 h. The second nickel introduction method was ionic exchange. The zeolite was exchanged with a nickel nitrate aqueous solution at 70–80 °C for 2 h, filtered, and washed with distilled water at 65 °C; then, it was dried at 120 °C for 12 h and calcined at 600 °C for 3 h in air.

2.2. Characterization of the catalysts

Specific surface area (SSA) of the materials were measured using nitrogen adsorption–desorption isotherms (BET method) in a Micromeritics equipment (model GEMINI 2375). Prior to the analysis, the catalysts (250 mg) were first treated at 60 °C for 1 h. Then, the catalyst was transferred to the reactor and outgassed under vacuum ($P < 50$ Torr) at 300 °C for 1 h. Adsorption–desorption experiments were performed with nitrogen at the temperature of liquid nitrogen. The equation of Brunauer–Emmett–Teller (BET) was used in the range of relative pressure (P/P_0) between 0.06 and 0.21 for SSA calculation.

Brönsted acid sites quantification by H/D isotope exchange technique [27] was performed in a grease-free, glass system equipped with a U-shaped reactor. The temperature was controlled with a thermocouple placed in the catalytic bed, while the gas flow was regulated with a Brooks 5850E mass flow controller. The Ni-modified catalyst (300 mg) was first activated under dry air flow (40 mL/min) at 450 °C for 1 h to desorb the water present in the void volume but without dehydroxylation of the framework. The temperature of the catalyst was then lowered to 200 °C for deuteration. Scheme 1 describes the different H/D steps involved.

At first, the catalyst deuteration was performed by passing dry N_2 through a U-shaped tube containing D_2O (about 0.05 g) at room temperature at 40 mL/min. and then sweeping through the catalyst for one hour. Excess of D_2O was removed by flushing dry N_2 at 200 °C during 90 min.

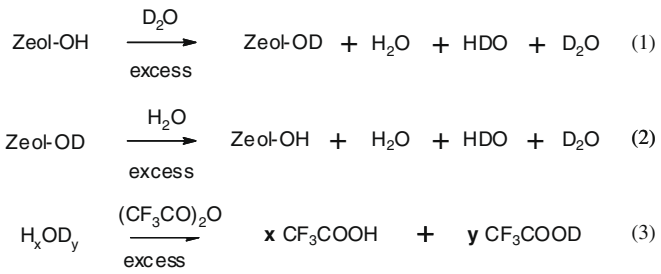

Scheme 1. Set of the H/D exchange steps between H_2O/D_2O and the OH groups of the zeolite.

Then, the deuterated catalyst (Zeo-OD) was back-exchanged (Eq. (2)) at 200 °C for 1 h by sweeping 40 mL/min of 3% of H_2O in N_2 stream. This step was necessary since the trifluoroacetic anhydride contains 0.11 mmol of trifluoroacetic acid per gram of anhydride as controlled in blank experiment. For this reason, it is warranted to titrate the Brönsted sites by using the anhydride with the partially exchanged water obtained after the last step (Eq. (2) in Scheme 1).

The partially exchanged water described by step two in Scheme 1 was collected in a U-tube cooled at −117 °C and weighted. Then, it was allowed to react with trifluoroacetic anhydride (in two-fold excess). The acid solution thus obtained was transferred under argon to a NMR tube for analysis. The spectra were recorded on a Bruker AM400 spectrometer (400 MHz) after an addition of a $CDCl_3$ (10 wt%)/$CHCl_3$ mixture as reference. The integration of CF_3COOH and CF_3COOD on both ^1H and ^2H spectra allows an accurate quantification of the H/D content of the sample. The acid site density was then calculated based on the H/D ratio measured and the mass of H_xOD_y collected.

The temperature-programed reduction (TPR) was performed in a glass reactor as reported elsewhere [28]. The profile was obtained under flow of 60 mL/min of a mixture of 1.5% H_2 in argon. Hydrogen consumption was monitored from room temperature up to 1000 °C with a heating rate of 10 °C/min and staying at this temperature for 1 h. The measurements were monitored on-line by mass spectrometry (MKS able to measure $m/z = 100$).

Measurements of XANES and EXAFS were carried out at the D08B XAS beamline at the National Laboratory of Synchrotron Radiation, operating at 1.37 GeV, with maximum ring current of 120 mA. The synchrotron radiation beam was monochromatized by a Si (2 2 0) double crystal. The spectra were collected in the K edge of Ni (8333 eV) in the fluorescence mode, using a Ge multi-element detector. Samples were pressed to form pellets and the spectra of metallic Ni foil (6 μm) and NiO powder were taken as a reference.

2.3. Cracking of n-hexane and ethane hydrogenolysis procedures

Before ethane hydrogenolysis, the catalyst was reduced at 500 °C for 2 h in a 10%v/v H_2/N_2 mixture with a flow rate of 60 mL/min (heating rate of 10 °/min). Then, the temperature was decreased to 430 °C and a reaction mixture of 10%v/v ethane in hydrogen passed through the reactor at 20 mL/min. The analysis of products was carried out on-line after 5, 10, and 15 min on stream, respectively, using a GC-2010 Shimadzu chromatograph. In all cases, only methane was observed as the product. The cracking of *n*-hexane was performed in the same experimental set-up. The catalyst was activated under nitrogen at 500 °C for 2 h. The flow was shifted to an 11%v/v of *n*-hexane in nitrogen mixture.

The products were injected on line after 3, 17, and 32 min on stream, respectively.

3. Results and discussion

3.1. Characterization of the catalysts

The metal content, the number of Brönsted acid sites and the SSA values for the different catalysts are given in Table 1. The metal introduction methodology is identified by a suffix: IMP denotes dry impregnation and EX corresponds to ionic exchange. The amount of metal is given in weight percent in the name of each catalyst. The catalysts 0.4NiEX, 1NiEX, and 1NiIMP showed a decrease of about 15% in SSA when compared to pristine zeolite. This effect was more pronounced for 4NiIMP and 6NiIMP zeolites with a loss of 20%. It is noteworthy that the SSA remained high for all-promoted materials whatever the Ni loading is. The total number of Brönsted acid sites is also shown in Table 1. As expected, pure H-ZSM-5 zeolite presents the highest concentration of hydroxyl groups, 1.58 mmol OH/g catalyst. The catalyst 0.4NiEX showed the value 1.32 mmol OH/g, which is similar to the estimated one supposing that all nickel is distributed as compensation cation in the zeolite framework (1.32 mmol OH/g_{cat} = (1.58 – [mmol Ni exchange × 2]). Each Ni^{2+} compensating cation neutralizes two hydroxyl groups. The number of Brönsted acid sites determined via H/D titration is also in line with this measurement. Similarly, the 1NiEX catalyst exhibited 1.06 mmol OH/g_{cat}. This loss of 0.52 mmol OH/g_{cat} is still in agreement with a complete exchange of Ni present as Ni^{2+} species.

The 1NiIMP catalyst showed a decrease of its acid site density to 1.43 mmol OH/g_{cat}. This small difference of 0.15 mmol OH/g suggests that the 1NiIMP catalyst has only 50% of nickel distributed as ionic species in the zeolite channels. The 4NiIMP zeolite exhibited 1.24 mmol OH/g_{cat}. This value also supported the presence of nickel oxide particle. Hence, from the relative amount of Ni that is not participating as compensation cations, it may be concluded that the tendency to form nickel oxide is therefore enhanced at higher metal loading.

TPR profiles are presented in Fig. 1. In all TPR experiments, all nickel was reduced from Ni^{2+} to Ni^0. Hydrogen consumption was separated in two temperature zones, which are presented in terms of percentage of total hydrogen consumption in Table 2. The low temperature reduction zone corresponds to the region between 400 °C and 740 °C. The high temperature zone is between 740 °C and 1000 °C. The 1NiEX catalyst showed only 11% of the total consumption of hydrogen at high temperature, while the 1NiIMP presents the same amount of hydrogen consumption at low and high temperatures (Table 2). These results are in agreement with the titrations of Brönsted acid sites (H/D exchange), which supported that 50% of nickel is distributed as compensation cations in the zeolite framework. These nickel species are probably reduced at temperatures higher than those required for reducing nickel oxide particles. Pawelec et al. proposed that nickel distributed as compensation cations were reduced above 630 °C, whilst the reduction of nickel oxide started around 500 °C [29]. While raising the nickel amount via impregnation procedure, 4NiIMP and 6NiIMP catalysts, the percentage of hydrogen consumption at high temperature decreased, whereas the amount of hydrogen consumed at low temperature was enhanced.

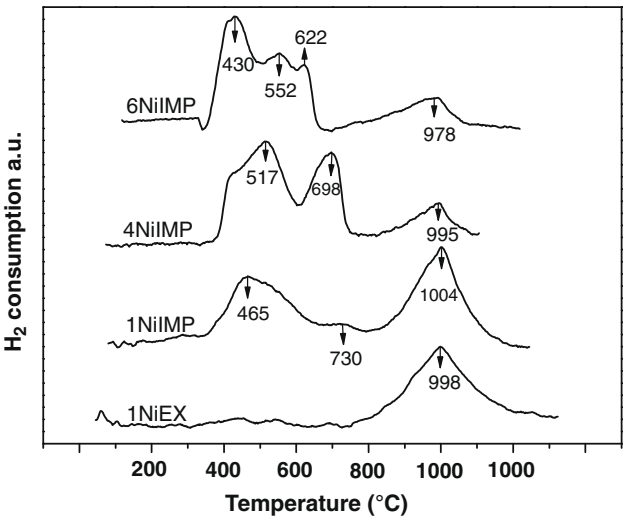

Fig. 1. TPR profiles for nickel ZSM-5 catalysts, nickel introduced by dry impregnation (IMP) and by ionic exchange (EX).

Table 2
Relative hydrogen consumption during TPR measurement at low and high temperature for nickel introduced by either dry impregnation method (IMP) or by ionic exchange method (EX). All catalysts exhibited a complete nickel reduction.

Catalyst	% Ni	
	Low temperature	High temperature
1NiEX	11	89
1NiIMP	50	50
4NiIMP	87	13
6NiIMP	84	16

Low temperature: 430–470 °C, 520–560 °C, and 630–720 °C.
High temperature: 1000 °C.

To summarize, nickel introduced by means of impregnation technique, up to 0.4% Ni wt/wt, led to a metal distribution exclusively as compensation cations of the zeolite framework. While further raising the metal content, the formation of metal oxide becomes favored. Based on earlier studies, the low temperature contribution can be separated in three domains as follows: (i) between 430 and 470, (ii) between 520 and 560, and (iii) between 630 and 720 °C. The former peak corresponds to the reduction of NiO particle [30]. The latter two peaks can probably be ascribed not only to small nickel particle but also to some nickel oligomeric species present in the zeolite channels as already observed for Mo-ZSM-5 species [31].

The EXAFS profiles for all catalysts are presented in Figs. 2–4. The catalysts containing nickel introduced by ionic exchange 0.4NiEX; 1NiEX and the catalyst 0.4NiIMP exhibited similar profiles. Exclusively neighbors (oxygen atoms) located in the first sphere of coordination were observed. Consequently, nickel is

Table 1
Metal content, surface area (estimated by BET method), and number of Brönsted acid sites of as-prepared Ni-ZSM-5 catalysts. Both families of catalysts were presented, IMP means nickel introduced by dry impregnation, EX means nickel introduced by ionic exchange.

Catalyst	ZSM-5	0.4NiIMP	0.4NiEX	1NiEX	1NiIMP	4NiIMP	6NiIMP
BET (m^2/g)	392	342	334	340	332	319	316
mmol of OH/g cat.	1.58	0.90	1.32	1.06	1.43	1.24	–
Metal amount (%)	0	0.37	0.31	0.83	1.00	3.65	6.00

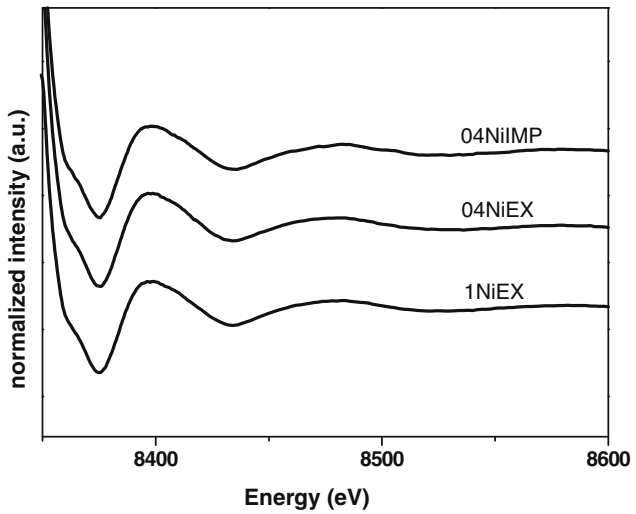

Fig. 2. EXAFS profiles in normalized energy for: 04NiEX, 1NiEX, 4NiEX (nickel introduced by ionic exchange method), and the 04NiIMP (nickel introduced by dry impregnation).

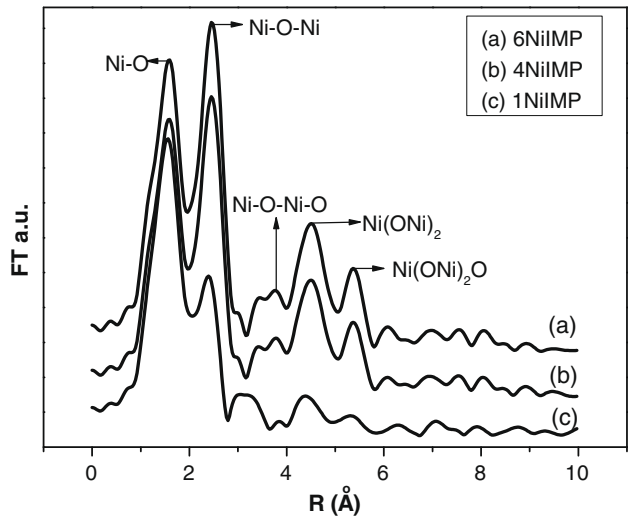

Fig. 3. EXAFS profiles in normalized R (k^{-2}) for: 1NiIMP, 4NiIMP, and 6NiIMP (nickel introduced by dry impregnation).

predominantly distributed as compensation cation for these catalysts (Fig. 2). Raising the nickel amount in impregnated samples led to the appearance of both second and third coordination spheres. This contribution increases from the 1NiIMP catalyst to the 4NiIMP and 6NiIMP catalysts (Fig. 3). The same features were previously observed for nickel on USY zeolite [32]. In addition, a thermal treatment under hydrogen led to the sintering of Ni particles on ZSM-5 [23]. The bond distance between these nearest neighbors is in the range with the ones observed in nickel oxide. Hence, in agreement with the TPR results, these EXAFS measurements indicate that besides Ni forms Ni^{2+} cations distributed as counter cations in the zeolites framework, small NiO particles are present in the impregnated catalyst. The nickel oxide exhibits Fm3 m cubic geometry and presents two main peaks in the EXAFS spectrum. The first peak, around 1.60 Å refers to Ni–O distance, being the first neighbor. The second one, located at 2.54 Å, corresponds to Ni–O–Ni distance [13,27]; it is noteworthy that up to five neighbors were observed (Fig. 3). The EXAFS results for 1NiEX catalyst and for 6NiIMP could be used to simulate nickel distribution

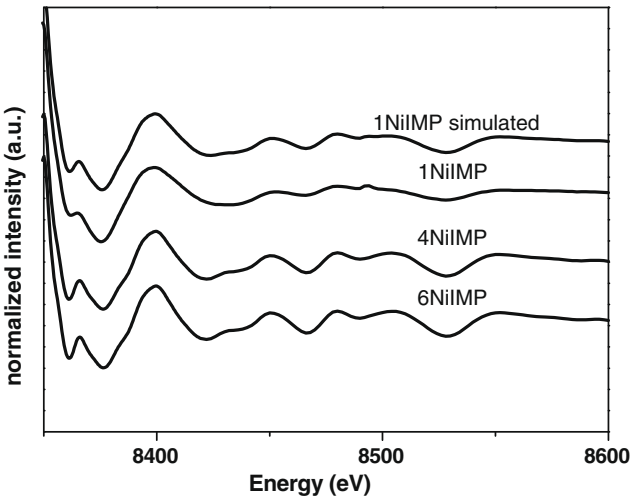

Fig. 4. EXAFS profiles in normalized energy for: 1NiIMP, 4NiIMP, 6NiIMP (nickel introduced by dry impregnation), and 1NiIMP simulated.

in the 1NiIMP catalyst profile. A reasonable simulation was carried out by using a weight of 0.5 for each profile, as presented in Fig. 4. This result is in line with the given values from the titration of remaining hydroxyl groups per gram as well as the TPR measurements. Hence, this corroborates that 50% of the nickel present in 1NiIMP catalyst is distributed as particle and 50% remains distributed as compensation cation.

Table 3 presents the results of ethane conversion used as a model reaction performed after reduction of the catalyst. This structure sensitive reaction allowed the discrimination between nickel particle formation and isolated species, or nickel present as compensation cations. The 0.4NiEX, 0.4NiIMP, and 1NiEX (exchanged catalysts) did not exhibit any hydrogenolysis activity while the other catalysts presented increasing conversion as the amount of nickel was raised, thus suggesting nickel distribution as NiO increases. It is important to point out that nickel dispersion before and after reduction is probably not the same. Nevertheless, one may still use the information in order to compare the nickel distribution in the catalyst.

3.2. Cracking of n-hexane

3.2.1. Observations

The catalysts prepared after calcination but without pre-reduction were tested in the *n*-hexane cracking at 500 °C (Fig. 5). The reaction rate is presented as a function of alkane conversion (mmol of *n*-hexane/g cat. min). The activity value is an average between 17 and 32 min on stream. These two values differ less than 5% regardless of the nickel presence in the ZSM-5. Consequently, it was considered that the activity was measured under steady-state conditions. A slight decrease in the activity was observed for nickel-exchanged catalysts when compared to parent HZSM-5 zeolite. Impregnated catalysts exhibited a larger decrease in the catalytic activity. The catalysts were not compared at very short time on stream. Consequently, the lower activity for nickel-impregnated catalyst could be probably ascribed to coke formation on nickel particles [33], although some effects on *n*-hexane accessibility cannot be totally ruled out.

As stated in the experimental section, the selectivity toward the different hydrocarbons was compared at similar conversion (7–11%). A large number of products were observed in the *n*-hexane cracking reaction. In comparison to non metal-doped acidic zeolite, nickel introduction led to an increase in the amount of alkenes, mainly ethylene, butene, and pentene. Fig. 6 shows the selectivity

Table 3
Ethane hydrogenolysis activity for Ni-ZSM-5 bifunctional catalysts, both methods of nickel introduction are presented: dry impregnation (IMP) and ionic exchange (EX).

Catalyst	6NiIMP	4NiIMP	1NiIMP	1NiEX	0.4NiIMP	0.4NiEX
Conversion (%)	77	67	10	0	0	0
Rate (mmol/g min)	1893	1647	245	0	0	0

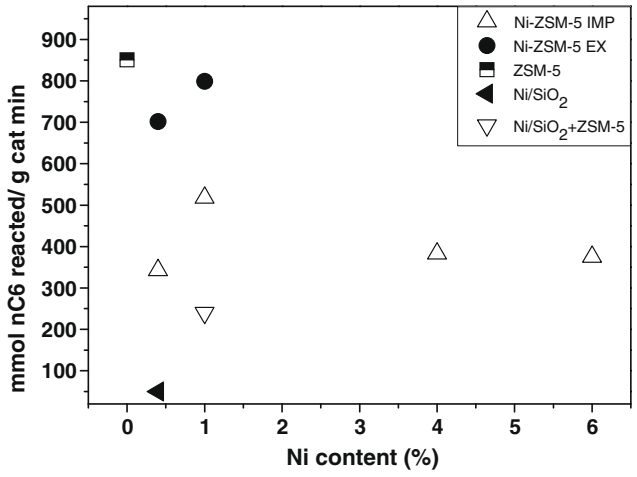

Fig. 5. *n*-Hexane cracking activity for both families of Ni-ZSM-5 catalysts, nickel introduced by dry impregnation (IMP), and by ionic exchange (EX).

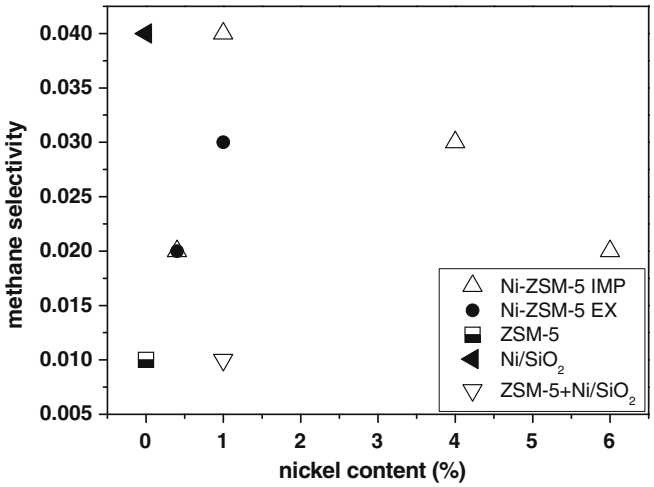

Fig. 7. Methane selectivity of nickel ZSM-5 catalysts, nickel introduced by dry impregnation (IMP) and by ionic exchange (EX).

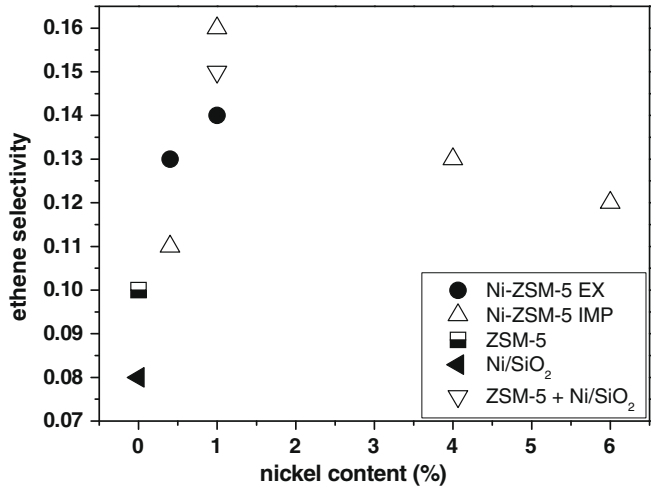

Fig. 6. Ethene selectivity of nickel ZSM-5 catalysts, nickel introduced by either dry impregnation (IMP) or ionic exchange (EX).

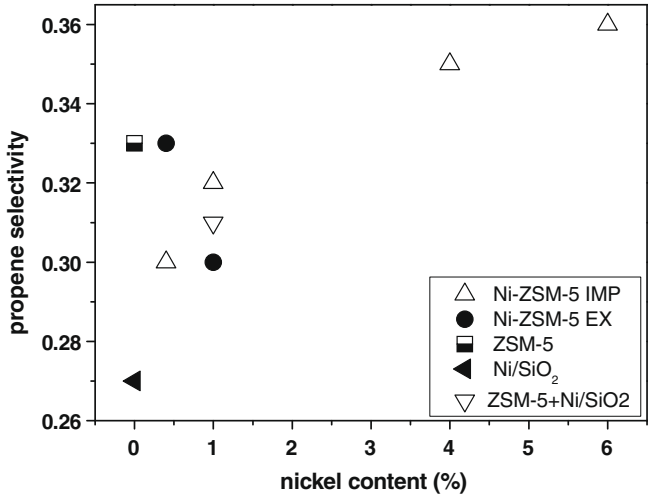

Fig. 8. Propene selectivity of nickel ZSM-5 catalysts, nickel introduced by dry impregnation (IMP) and by ionic exchange (EX).

toward ethylene. All nickel catalysts produced a higher ethylene yield when compared to pristine H-ZSM-5. The selectivity toward methane followed the same tendency after nickel introduction (Fig. 7). However, this effect was less pronounced than the increase in ethylene selectivity. Fig. 8 shows that propylene selectivity remains nearly the same for all catalysts in agreement with a protolytic activation of the alkane [34].

3.2.2. Interpretation for increase in olefin production

The different reaction pathways occurring in *n*-hexane cracking over ZSM-5 zeolite have been reported several times in the literature [35,36]. According to this reaction sequence, β-scissions should produce equal amounts of propane and propylene and also equal amounts of total butanes (*n*-butane and isobutane) and ethylene. The former ratio is close to one on parent HZSM-5 zeolite and also on 1NiEX catalyst. Propylene and ethylene could also be formed by a protolysis mechanism on zeolite acid sites, according to the σ-basicity rule developed by Olah [37].

However, after nickel introduction by impregnation method, the amount of propylene is higher than propane. The ethylene/butane ratio remains also higher than one for 1NiEX catalyst, thus indicating that the presence of nickel induces secondary cracking reactions. For instance, butenes and pentenes can re-adsorb on ZSM-5 acid sites and react further, and hence increase ethylene selectivity. Indeed, these olefins formed on nickel sites may either react with zeolite acid sites (forming carbenium species) or react with carbenium species, as shown in the carbenium cycle, Fig. 9.

The chemistry of olefins on solid acids is well described in the literature [38,39]. In zeolites, olefins are easily protonated by a Brönsted acid site, following the σ-basicity rule, thus forming a

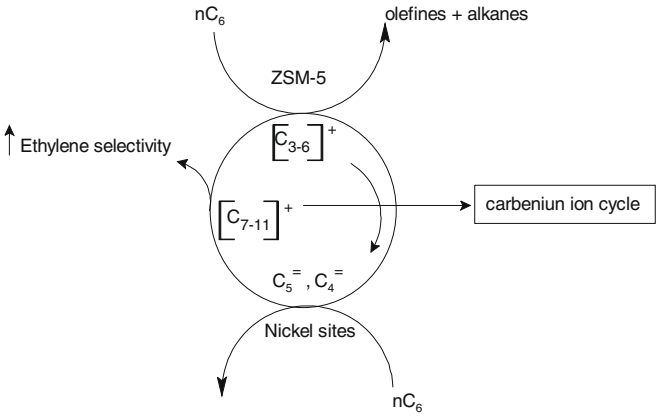

Fig. 9. Nickel effect on the Carbenium ion cycle.

carbenium ion [37]. These positive charged species are probably in equilibrium with their corresponding olefin precursor. Increasing the olefin amount may improve the bimolecular reactions [40,41] and thus larger carbenium ion could be formed within zeolite channels or cages. Ethylene could therefore be favored via beta cracking reactions of these larger carbenium ions since large molecules hardly diffuse in the channels of the ZSM-5 zeolite.

The effect of nickel was further investigated and compared to nickel supported on pure silica Ni/SiO_2 catalyst (0.47 wt% Ni, SSA = 50 m^2/g and 0.54 m^2/g of nickel superficial area, average particle diameter 5.4 nm, prepared by wetness impregnation) [42]. It is important to mention that the Ni/SiO_2 catalyst was only calcined and not reduced before the *n*-hexane model test. The results for Ni/SiO_2 catalyst, pure or mixed with ZSM-5, are summarized in Table 4. The Ni/SiO_2 catalyst showed a very low reaction rate (51 mmol of alkane converted/g cat. min). This reactivity was approximately 20 times lower than the one achieved with pure zeolite. The propylene and ethylene selectivity formed on Ni/SiO_2 catalyst was 27 and 8%, respectively. Besides C_4 and C_5 olefins were also formed.

One can compare the yields (=rate activity × selectivity, expressed in g of *n*-hexane/g cat. min related for several products) in ethylene, propylene, butenes, and pentenes at 10% *n*-hexane conversion. For Ni/SiO_2, the yields were: 4, 19, 19, and 1.5 (g nC_6/g cat. min), respectively. For 1NiIMP catalyst the yields were: 166, 83, 62, and 19 (g *n*-hexane/g cat. min). It is therefore expected that only a small contribution comes from Ni/SiO_2 catalyst for the products formed in the mixture of catalysts.

This catalyst mixture (Ni/SiO_2 + ZSM-5) showed high ethylene selectivity compared to pristine catalyst while propylene selectivity remained similar to pure zeolite. These selectivity values were similar to the ones presented by the 1NiIMP and 1NiEX catalysts.

Table 4
n-Hexane activity and selectivity: comparison mixtures of nickel on silica and pure ZSM-5 with both 1% Ni ZSM-5 catalyst (1NiIMP- nickel was introduced by impregnation method and 1NiEX - nickel was introduced by ionic exchange method).

Catalyst	ZSM-5	Ni/SiO_2	1NiIMP	1NiEX	ZSM-5 + Ni/SiO_2 (1%)
Rate (mmol nC_6/g cat. min)	940	51	519	799	738[a]
Conversion (%)	7	7	10	10	7
Ethylene selectivity (%)	10	8	16	14	15
Propylene selectivity (%)	33	27	32	30	31
Methane selectivity (%)	1	4	4	3	1

[a] The value of the rate was calculated based on the mass of the pure zeolite (ZSM-5).

The improvement in ethylene selectivity is not a simple addition of ethylene formed on nickel and acid sites. It seems that nickel provides the olefin precursor that can be cracked by acid sites. This enhances ethylene formation as shown in the Fig. 9.

Generally, a bifunctional catalyst contains both acid and metallic sites where the metal is in zero oxidation state. Although Ni-ZSM-5 catalysts were not previously reduced before *n*-hexane evaluation (in agreement with more realistic catalysts condition in the FCC process), metallic nickel sites could still be formed via a partial reduction by *n*-hexane during the catalytic test. However, these metallic sites would contribute to hydrogenolysis. On the other hand, isolated Ni positive species present in the zeolite can interact with CO molecules [43]. In addition, these species are probably able to react with hydrocarbons via attack of alkane σ-bond-promoting dehydrogenation reactions. Since nickel sites and acid sites are in close contact, the dehydrogenation products formed on nickel sites reacted sequentially in the carbenium cycle. In this way, a new type of bifunctional catalyst is produced. This can be readily achieved by the ion exchange method, which permits a high dispersion of Ni cations and improved access of olefins to the acid sites.

4. Conclusions

Calcined nickel ZSM-5 zeolite catalyst improves the selectivity toward light olefins in cracking reaction when compared to pristine zeolite. A careful examination of nickel supported on silica catalyst (mixtured or not with ZSM-5) and ZSM-5 confirmed that the bi-functional catalysis occurred on calcined Ni-ZSM-5 samples. This bifunctional catalysis can be optimized by the use of proper metal introduction methodology.

Nickel was introduced into ZSM-5 zeolite by wetness impregnation and by ionic exchange method. The later improves the formation of light olefins. At low nickel loading (0.4 wt%), nickel is distributed as compensation cation for both methods of metal introduction. The introduction of nickel by wetness impregnation (1% wt/wt) led to its equal distribution as compensation cation of the zeolite structure and as NiO particle. While increasing the nickel amount by wetness impregnation, the formation of nickel oxide particle was favored in contrast to its distribution as compensation cations.

Finally, precise information about the nickel location as a function of the preparation method could be used to design the catalyst in order to enhance light olefin production.

Acknowledgments

The authors thank the LNLS for EXAFS and XANES at D08B XAS under project number D04B-XAFS1-6463 and are grateful to CNPq for fellowship.

References

[1] M. Lallemand, O.A. Rusu, E. Dumitriu, A. Finiels, F. Fajula, V. Hulea, Appl. Catal. A 338 (2008) 37.
[2] J.R. Sohn, Catal. Surveys Asia 8 (2004) 4.
[3] R.E. Roncolatto, L.Y. Lau, W.R. Gilbert, J. Gorne, BR Patent, BR 200305957-A, 2003, Petrobras Petroleo Brasil SA.
[4] G.A. Olah, G.K. Surya Prakash, A. Molnár, J. Sommer, Superacid Chemistry, John Wiley and Sons Inc., Hoboken, NJ, 2009, p. 501.
[5] A. Corma, Chem. Rev. 95 (1995) 559.
[6] C. Baes, R. Mesmer, The Hydrolysis of Cations, Robert E. Krieger Publishing Company, Malabar, FL, 1986, p. 246.
[7] A. Carrero, J.A. Calles, A.J. Vizcaino, Appl. Catal. A 327 (2007) 82.
[8] T. Mang, B. Breitscheldel, P. Polanek, Appl. Catal. 106 (1993) 239.
[9] V. Kazansky, A. Serykh, Microporous Mesoporous Mater. 70 (2004) 151.
[10] A. Khodakov, N. Barbouth, J. Oudar, J. Phys. Chem. B 101 (1997) 766.
[11] J.P. Tessonnier, B. Louis, S. Rigolet, M.J. Ledoux, C. Pham-Huu, J. Phys. Chem. B 110 (2006) 10390.

[12] M. Mihaylov, K. Hadjiivanov, D. Panayotov, Appl. Catal. A 51 (2004) 33.
[13] B.I. Mosqueda-Jiménes, A. Jentys, K. Seshan, J.A. Lercher, J. Catal. 218 (2003) 375.
[14] M. Bäumer, H.-J. Freund, Progr. Surf. Sci. 61 (1999) 127.
[15] P. Turlier, H. Praliaud, P. Moral, Appl. Catal. 19 (1985) 287.
[16] R. Burch, A.R. Flambard, J. Catal. 85 (1984) 16.
[17] A.S. Escobar, M.M. Pereira, R.D.M. Pimenta, L.Y. Lau, H.S. Cerqueira, Appl. Catal. A 286 (2005) 196.
[18] H.M.T. Oliveira, M.H. Herbst, H.S. Cerqueira, M.M. Pereira, Appl. Catal A 292 (2005) 82.
[19] A.S. Escobar, F.V. Pinto, H.S. Cerqueira, M.M. Pereira, Appl. Catal. A 315 (2006) 68.
[20] M. Boudart, G. Djega-Mariadassou, Kinetics of Heterogeneous Catalytic Reactions, Princeton University Press, Princeton, NJ, 1984.
[21] J.H. Sinfelt, J.L. Carter, D.J.C. Yates, J. Catal. 24 (1972) 283.
[22] J.L. Jiang, J.F. Yao, C.F. Zeng, L. Zang, N. Xu, Microporous Mesoporous Mater. 112 (2008) 450.
[23] A.S. Escobar, M.M. Pereira, H.S. Cerqueira, Appl. Catal. A 339 (2008) 61.
[24] A. Masalska, Catal. Today 65 (2001) 249.
[25] Y.L. Lam, D. Satamires, J. Gorne, J.C. Moreira Ferreira, J. da Silva, European Patent Office Application, 05075770.7 (2005).
[26] B.R. Mitchel, Ind. Eng. Chem. Res. Dev. 19 (1980) 209.
[27] B. Louis, S. Walspurger, J. Sommer, Catal. Lett. 93 (2004) 81.
[28] L.T. Santos, E.B. Pereira, N. Homs, J. Llorca, P.R. de la Piscina, M.M. Pereira, Catal. Today 78 (2003) 459.
[29] B. Pawelec, R. Mariscal, R.M. Navarro, J.M. Campos-Martin, J.L.G. Fierro, Appl. Catal. A 262 (2004) 155.
[30] M. Iwamoto, Catal. Surv. Asia 12 (2008) 28.
[31] J.P. Tessonnier, B. Louis, S. Rigolet, M.J. Ledoux, C. Pham-Huu, Appl. Catal. A 336 (2008) 79.
[32] J.Y. Carriat, M. Che, M. Kermarec, M. Verdaguer, A. Michalowicz, J. Am. Chem. Soc. 120 (1998) 2059.
[33] S.H. Seok, S.H. Choi, E.D. Park, J. Catal. 209 (2002) 6.
[34] A. Brait, K. Seshan, J.A. Lercher, Appl. Catal. A 169 (1998) 299.
[35] R.R. Pinto, P. Borges, F. Lemos, F. Ramôa Ribeiro, Appl. Catal. A 272 (2004) 23.
[36] H.M. Liu, G.H. Kuehl, I. Halasz, J. Catal. 249 (2003) 175.
[37] G.A. Olah, A. Burrichter, G. Rasul, J. Sommer, J. Am. Chem. Soc. 118 (1996) 10423.
[38] Y.V. Kissin, Catal. Rev. 43 (2001) 85.
[39] S.M. Babitz, B.A. Willians, J.T. Miller, R.Q. Snurr, W.O. Haag, H.H. Kung, Appl. Catal. A 179 (1999) 71.
[40] G. Zhao, J. Teng, Y. Tang, J. Catal. 248 (2007) 29.
[41] L.H. Nguyen, T. Vazhnova, D.B. Lukyanov, Chem. Eng. Sci. 61 (2001) 5881.
[42] J.M. Richardson, C.W. Jones, J. Mol. Catal. A 297 (2009) 125.
[43] K. Hadjiivanov, H. Knozinger, M. Mihaylov, J. Phys. Chem. 106 (2002) 2618.